



Heriot-Watt University
Research Gateway

A pressure-based estimate of synthetic jet velocity

Citation for published version:

Persoons, T & O'Donovan, TS 2007, 'A pressure-based estimate of synthetic jet velocity', *Physics of Fluids*, vol. 19, no. 12, 128104, pp. -. <https://doi.org/10.1063/1.2823560>

Digital Object Identifier (DOI):

[10.1063/1.2823560](https://doi.org/10.1063/1.2823560)

Link:

[Link to publication record in Heriot-Watt Research Portal](#)

Document Version:

Early version, also known as pre-print

Published In:

Physics of Fluids

General rights

Copyright for the publications made accessible via Heriot-Watt Research Portal is retained by the author(s) and / or other copyright owners and it is a condition of accessing these publications that users recognise and abide by the legal requirements associated with these rights.

Take down policy

Heriot-Watt University has made every reasonable effort to ensure that the content in Heriot-Watt Research Portal complies with UK legislation. If you believe that the public display of this file breaches copyright please contact open.access@hw.ac.uk providing details, and we will remove access to the work immediately and investigate your claim.

A pressure-based estimate of synthetic jet velocity

Tim Persoons^{a)} and Tadhg S. O'Donovan

Mechanical and Manufacturing Engineering, Parsons Building, Trinity College, Dublin 2, Ireland

(Received 30 August 2007; accepted 30 October 2007; published online 18 December 2007)

Synthetic jets are used for active flow control and enhanced heat transfer, and are typically generated by an orifice connected to a cavity with movable diaphragm actuator. Low-power operation is achieved by matching actuator and Helmholtz resonance frequencies. This brief communication presents an analytical model derived from simplified gas dynamics, for estimating the synthetic jet velocity and actuator deflection, based on a cavity pressure measurement. Model closure is provided by a damping force in the orifice, which agrees with established pressure loss correlations for steady flow through short ducts. The model is validated against experimental data obtained for an axisymmetric synthetic jet. The valid frequency range extends from zero, over the Helmholtz resonance frequency, up to a geometry-dependent limit frequency. This model presents a reference against which synthetic jet velocity can be calibrated. © 2007 American Institute of Physics.

[DOI: 10.1063/1.2823560]

Synthetic or zero-net mass flux jets are being studied in various fields of fluid dynamics, from active flow control to enhanced heat transfer. A synthetic jet is produced by the interaction of a train of vortices that form by successive ejection and suction of fluid across an orifice. The orifice flow is forced by periodic pressure variations, typically generated in a cavity with a movable diaphragm. Optimum efficiency is achieved by matching the mechanical resonance frequency of the actuator to the Helmholtz resonance frequency of the gas dynamic cavity-orifice system.

An unconfined synthetic jet flow is characterized by two parameters: the stroke length L_0/d and the Reynolds number $Re=U_0d/\nu$, where d is the orifice hydraulic diameter, $L_0=\int_0^{T/2}U(t)dt$, T is the oscillation period, $U_0=L_0/(T/2)$, and $U(t)$ is the area-averaged orifice velocity, although sometimes¹ the centerline velocity is used instead. L_0/d is inversely proportional to a Strouhal number, since $L_0/d = \frac{1}{2}(fd/U_0)^{-1}$.

As such, setting the operating point of a synthetic jet requires knowledge of the jet velocity, which is only measurable using advanced methods such as laser-Doppler anemometry, particle image velocimetry, and hot-wire anemometry. Therefore, a calibration is typically performed to determine the relationship between the synthetic jet velocity and the actuator input voltage. However, this relationship is subject to actuator degradation and other external influences. To overcome this problem, some researchers^{1,2} suggest a calibration of velocity versus cavity pressure instead.

Smith and Glezer¹ indicate that for a pair of closely spaced synthetic jets, the velocity is influenced by the presence of the adjacent jet, particularly when the jets are driven out of phase. For that reason, they recommend a pressure-velocity calibration. Smith and Glezer² use a synthetic jet to deflect a primary steady jet. A pressure-velocity calibration is used to characterize the synthetic jet, recording several calibration curves for different frequencies. Smith and Glezer²

note that changes in the primary flow affect the pressure-velocity relationship.

Crittenden and Glezer³ describe a compressible flow synthetic jet based on a piston-crank arrangement, characterizing the jet performance with cavity pressure measurements. A numerical quasistatic model is solved to predict the pressure-velocity relation, assuming adiabatic compression/expansion in the cavity and one-dimensional compressible isentropic flow in the orifice, neglecting friction and additional losses [see Eq. (11)]. The model agrees satisfactorily with measured pressure data. Lockerby and Carpenter⁴ also propose a computational approach for predicting the pressure-velocity relationship for microscale synthetic jets. The numerical model assumes isothermal compression/expansion in the cavity and laminar fully developed compressible flow in the orifice. Rathnasingham and Breuer⁵ propose a simple analytical model similar to the one used in this brief communication, except their model assumes inviscid orifice flow without losses, satisfying the Bernoulli principle.

Contrary to numerical approaches,^{3,4} this brief communication describes an analytical model based on simplified gas dynamics for estimating the synthetic jet velocity and actuator deflection, based on a cavity pressure measurement. The model is semi-empirical and requires a single coefficient K , which is shown to correspond to a steady flow pressure loss coefficient. The model is applicable to single or adjacent synthetic jets issuing in quiescent fluid. In nonquiescent fluid operation, the model accuracy should be verified.²

The relations among actuator deflection x_d , cavity pressure p , and jet velocity U are described by two ordinary differential equations. Firstly, the conservation of mass in the cavity, combined with the ideal gas law and assuming adiabatic compression/expansion, yields

$$\frac{1}{\gamma p_0} \frac{dp}{dt} = \frac{A_d}{V} \frac{dx_d}{dt} - \frac{A}{V} U, \quad (1)$$

where γ is the specific heat ratio, A_d is the actuator deflection area, V is the cavity volume, and A is the orifice cross-

^{a)}Electronic mail: tim.persoons@tcd.ie.

sectional area. The varying relative pressure p is assumed small compared to the absolute pressure p_0 . Secondly, the conservation of momentum in the orifice is

$$m \frac{dU}{dt} + F_D(U) = pA, \quad (2)$$

where $F_D(U)$ represents a damping force, and $m = \rho AL'$ is the mass of gas in the orifice. The effective length L' is the sum of the geometric length L and end corrections $L' - L = 2\beta d$, where $\beta = 0.425$ for a sharp-edged circular orifice.⁶ Two options were considered for the damping force F_D :

- (i) $F_D(U) = cU$ (linear damping),
- (ii) $F_D(U) = KA\rho U|U|/2$ (nonlinear damping),

where c is a viscous damping coefficient and K is a pressure loss coefficient.

Eliminating the pressure p from Eqs. (1) and (2) yields

$$m \frac{dU}{dt} + F_D(U) + k \int_{t_0}^t U dt = \frac{A_d}{A} k x_d, \quad (3)$$

where k is the cavity compressibility, and $k = \gamma p_0 A^2 / V$. Equation (3) describes the motion of a damped harmonic oscillator with eigenfrequency $\omega_0 = \sqrt{k/m} = (a/L') \sqrt{AL'/V}$, where a is the speed of sound. To estimate the synthetic jet velocity U , Eq. (2) is used rather than Eq. (3), since the pressure p is easier to measure than the deflection x_d .

Two sets of analytical relations are now derived for U/p and x_d/p , for linear and nonlinear damping. All variables are assumed to be harmonic functions (this assumption is justified based on the experimental data shown in Fig. 1):

$$x_d = x_d^* \sin \omega t, \quad p = p^* \sin(\omega t + \phi_p), \quad (4)$$

$$U = U^* \sin(\omega t + \phi_U).$$

Firstly, combining Eqs. (4) and (2) with $F_D = cU$ yields

$$m\omega U^* \cos(\omega t + \phi_U) + cU^* \sin(\omega t + \phi_U) = p^* A \sin(\omega t + \phi_p), \quad (5)$$

which results in a magnitude and phase equality

$$\frac{\rho a U^*}{p^*} = \sqrt{\frac{V}{AL'}} \left[\sqrt{\left(\frac{\omega}{\omega_0}\right)^2 + 4\zeta^2} \right]^{-1} \quad (6)$$

and $\phi_U - \phi_p = -\arctan\left(\frac{\omega/\omega_0}{2\zeta}\right)$,

where ζ is the critical damping coefficient: $\zeta = c/(2m\omega_0)$. Secondly, combining Eqs. (4) and (2) with $F_D = KA\rho U|U|/2$ and approximating $|\sin \theta| \sin \theta \cong \sin \theta$ yields

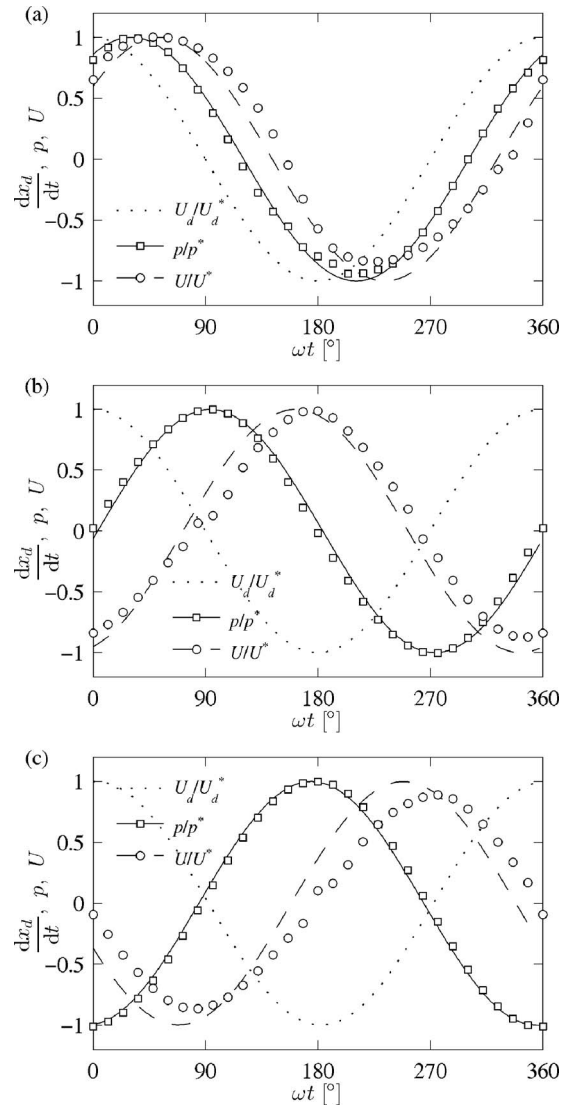


FIG. 1. Phase-locked cavity pressure p and jet velocity U for (a) $\omega = 0.26\omega_0$, (b) $\omega = \omega_0$, and (c) $\omega = 2.6\omega_0$.

$$m\omega U^* \cos(\omega t + \phi_U) + \frac{1}{2}KA\rho U^{*2} \sin(\omega t + \phi_U) = p^* A \sin(\omega t + \phi_p), \quad (7)$$

which results in

$$\frac{\rho a U^*}{p^*} = \sqrt{\frac{2V}{AL'}} \times \left[\sqrt{\left(\frac{\omega}{\omega_0}\right)^2 + \sqrt{\left(\frac{\omega}{\omega_0}\right)^4 + K^2 \left(\frac{V}{AL'}\right)^2 \left(\frac{p^*}{\rho a^2}\right)^2}} \right]^{-1} \quad (8)$$

and $\phi_U - \phi_p = -\arctan\left(\frac{\omega/\omega_0}{\frac{1}{2}KU^*/(\omega_0 L')}\right)$.

In the limit case without damping ($c=0$; $K=0$), Eqs. (6) and (8) both reduce to $\rho a U^*/p^* = \sqrt{V/(AL')} [\omega/\omega_0]^{-1}$, and the jet velocity lags the cavity pressure by 90° .

Irrespective of the damping force, the actuator deflection amplitude can be determined from Eq. (1):

$$\frac{kx_d^*}{p^* A} = \frac{A}{A_d} \left[1 + \left(\frac{\rho a U^* \omega_0 L' \omega_0}{p^* a \omega} \right)^2 - 2 \frac{\rho a U^* \omega_0 L' \omega_0}{p^* a \omega} \sin(\phi_U - \phi_p) \right]^{1/2}, \quad (9)$$

where $\rho a U^*/p^*$ and $\phi_U - \phi_p$ are given by Eqs. (6) or (8) for linear or nonlinear damping, respectively.

Equations (6), (8), and (9) describe transfer functions of jet velocity U and actuator deflection x_d , with respect to the measured cavity pressure p . In acoustical terms, $\rho a U^*/p^*$ represents the dimensionless admittance, where ρa denotes the characteristic impedance of the medium.

The established pressure-velocity relationships of Eqs. (6) and (8) contain damping coefficients c ($c=2\zeta m\omega_0$) and K . These can be determined by calibrating the synthetic jet with a reference velocity measurement. The current research employs constant temperature hot-wire anemometry (HWA) to validate the model, and determine the damping coefficients. In the final part of the paper, the value of K is compared to the pressure loss for steady flow through the orifice. The synthetic jet used for the validation consists of a loudspeaker-actuated cylindrical cavity (volume $V=115 \text{ cm}^3$) with a sharp-edged circular orifice ($d=5 \text{ mm}$, $L=10 \text{ mm}$), resulting in a calculated Helmholtz frequency ω_0 of 191 Hz at 25 °C. A high-pressure microphone (G.R.A.S. 40BH, 0.5 mV/Pa) is used to measure the cavity pressure p . Both velocity and pressure measurements feature a bandwidth in excess of 20 kHz. An uncertainty of 5% is obtained for the phase-locked measurements.

Figure 1 shows some selected phase-locked measurements, where Figs. 1(a)–1(c) represent three ratios of frequency to Helmholtz resonance frequency. Each plot shows $U_d=dx_d/dt$ (dotted line), cavity pressure p (square markers), and jet velocity U (circular markers). All quantities are normalized with their respective amplitude U_d^* , p^* and U^* , and the HWA signal has been de-rectified. The markers represent measurements. The solid line is a sine wave fitted to the pressure measurements. The dashed line is based on the nonlinear model in Eq. (8). At low frequency, the jet velocity U follows the volumetric displacement rate of the actuator U_d . The phase angles ϕ_p and ϕ_U increase with frequency, yet the phase difference $\phi_U - \phi_p$ tends to a maximum of 90° above the resonance frequency.

In Fig. 2, the circular markers represent the experimental data for different synthetic jet operating conditions. The lines represent the models. Figure 2(a) presents the data as $(\rho a U^*/p^*)\sqrt{AL'/V}$ in decibels. For the undamped case, this quantity equals $(\omega/\omega_0)^{-1}$ (dotted line). Figure 2(b) shows the phase difference between velocity and pressure $\phi_U - \phi_p$. The dotted line corresponds to the phase lag of 90° between velocity and pressure in the undamped case. The wide range of the markers clearly indicates nonlinearity in the system. In selecting the operating conditions, a range of frequencies has been set while maintaining a constant pressure amplitude p^* . This is repeated for five pressure levels (20, 50, 100, 200, and 500 Pa). The dashed line in Fig. 2 represents the linear model in Eq. (6), which does not match the experimental data. The five solid lines represent the nonlinear model in Eq.

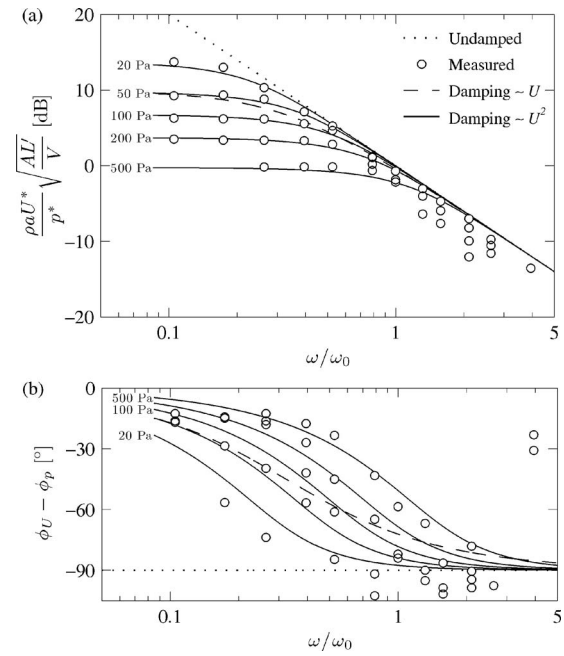


FIG. 2. Experimental validation of the pressure-velocity relationship using the proposed model, with linear and nonlinear damping described by Eqs. (6) and (8).

(8), for the same pressure levels used during the experiments. This model does show a good agreement to the experimental data, at least for $\omega \leq 1.5\omega_0$.

The linear and nonlinear models [Eqs. (6) and (8)] have each been least-squares fitted to the experimental data. This results in the following values for the damping coefficients: $K=1.46 \pm 0.13$ ($R^2=0.83$) and $\zeta=0.146 \pm 0.011$ ($R^2=0.44$). These values are specific to this synthetic jet. However, as discussed below, K is comparable to the pressure loss coefficient for steady flow through the orifice. As such, its value can be estimated for any geometry and operating conditions. However, this assumption has not been validated, since the current research is restricted to a single geometry.

The validation results in Fig. 2 demonstrate that nonlinear damping is appropriate. The model proposed by Lockery and Carpenter⁴ assumes fully developed laminar orifice flow, corresponding to linear damping. Rathnasingham and Breuer⁵ propose a nonlinear model, yet assume inviscid orifice flow without losses, satisfying the Bernoulli principle. This approach corresponds to $K=1$, whereas the above validation results yield a pressure loss coefficient $K>1$.

As Fig. 2 shows, U^*/p^* tends to a constant (yet amplitude-dependent) value for low frequencies, and the phase lag between velocity and pressure tends to zero. For high frequencies, the behavior tends to the undamped case. These trends are also observed in the experimental data, although the markers exhibit increasing scatter for $\omega > 1.5\omega_0$, which is due to limitations of the simplified gas dynamics.

In the simplified model, the cavity is considered a pure compliance without acoustic mass, and the orifice is considered a pure acoustic mass without compliance. Beranek⁶ describes the validity limits for these assumptions as a function of the wavelength $\lambda=2\pi a/\omega$. The largest dimension of the

cavity L_{cav} and the orifice length L should be smaller than $\lambda/16$. These criteria mark the upper validity limit for the model:

$$\omega < \frac{1}{16} \frac{2\pi a}{\max[L, L_{\text{cav}}]}. \quad (10)$$

The largest dimension of the jet cavity used for validating the model $L_{\text{cav}}=75$ mm. Equation (10) yields a limit frequency of 280 Hz ($\sim 1.5\omega_0$) for the cavity to act as a pure compliance. The orifice ($L=10$ mm) acts as a pure acoustic mass up to 2100 Hz ($\sim 11\omega_0$). The discrepancy in Fig. 2 between model and experimental data for $\omega > 1.5\omega_0$ can therefore be attributed to the complex pressure field in the cavity when exceeding the limit frequency.

For second-order damping, $F_D(U)=K\Delta p U/2$, where K represents a pressure loss coefficient. The question arises as to whether the value of K agrees with established pressure loss correlations. The pressure loss $K_s=\Delta p_s/(\rho U^2/2)$ for steady flow through an orifice of hydraulic diameter d and length L is comprised of four contributions,

$$K_s = K_f + K_d + K_c + K_e, \quad (11)$$

where K_f is the fully developed flow friction loss, K_d is the pressure loss due to boundary layer development, and K_c and K_e are, respectively, losses due to flow contraction and expansion at inlet and outlet of the orifice. Shah and London⁷ provide a correlation for the pressure loss in laminar flow, including the boundary layer development pressure loss,

$$K_f + K_d = \frac{f \text{Re} L^+ + K_\infty + 13.74C(L^+)^{-3/2}}{1 + C(L^+)^{-2}}, \quad (12)$$

where $f \text{Re}=64$, $K_\infty=1.25$, and $C=0.000212$ for a circular orifice. Equation (12) is valid for $L^+=(L/d)/\text{Re} > 2 \times 10^{-4}$. Kays and London⁸ provide data to determine the contraction and expansion loss. For flow through an isolated orifice, the expansion pressure loss $K_d=1$, and the contraction pressure loss is given by $K_c=(1-C_{c,0})+2(k_d^{\text{in}}-1)$, where $C_{c,0}=0.615$ and, assuming a uniform velocity profile, $k_d^{\text{in}}=1$.

For the orifice of the synthetic jet used in validating the model, $K_c+K_e=1.39$, which is velocity independent. However, the value of K_f+K_d obtained from Eq. (12) does depend on the Reynolds number. For a velocity range from 5 to 25 m/s (corresponding to the validation experiments), and K_s varies from 1.87 to 1.60. Synthetic jets typically feature a short orifice, where the main pressure loss contribution is due to contraction and expansion loss.

Measurements of the pressure loss in steady flow yield a value of $K_s=1.41 \pm 0.14$, which is slightly below the predicted range. However, it corresponds very well to the value obtained from the validation experiments ($K=1.46 \pm 0.13$).

In conclusion, an analytical model derived from simplified gas dynamics is presented to estimate synthetic jet ve-

locity and actuator deflection from the measured cavity pressure. Model closure is provided by a damping force to the gas motion in the orifice. The experimental validation results in Fig. 2 confirm a strong nonlinearity for frequencies below the Helmholtz resonance. The analytical model with second-order damping [Eq. (8)] is in good agreement with velocity data obtained using hot-wire anemometry. The simplified gas dynamic model is valid below and up to the Helmholtz resonance frequency. Above the resonance, the model remains valid up to the geometry-dependent limit frequency in Eq. (10). The model is semi-empirical, and requires the knowledge of the pressure loss coefficient K . The validation has shown that a nonlinear damping force is appropriate. In spite of the model's simplicity, it provides an accurate prediction of the actual synthetic jet velocity.

The model validation yields a pressure loss coefficient K for the specific synthetic jet (here, $K=1.46 \pm 0.13$). This value is comparable to known pressure loss correlations for steady flow in short ducts. Moreover, the value of K corresponds very well to the measured pressure loss in steady flow ($K_s=1.41 \pm 0.14$). This finding suggests that the proposed model does not require a velocity calibration, yet simply a measurement of the pressure loss coefficient for steady flow through the orifice.

Since the model is pressure based, it does not impose any restrictions on the nature of the actuator (e.g., loudspeaker, piezoceramic, piston), and is therefore applicable to many types of synthetic jet generators. The generic nature of the proposed model [Eq. (8)] allows the pressure-based estimation of the synthetic jet velocity for other jet designs, requiring only a limited calibration or even simply a pressure loss measurement for steady flow through the orifice.

The authors acknowledge the financial support of Enterprise Ireland (Grant No. PC/06/191). This work is performed in the framework of the Centre for Telecommunications Value-Chain Research (CTVR).

¹B. L. Smith and A. Glezer, "Vectoring of adjacent synthetic jets," *AIAA J.* **43**, 2117 (2005).

²B. L. Smith and A. Glezer, "Jet vectoring using synthetic jets," *J. Fluid Mech.* **458**, 1 (2002).

³T. M. Crittenden and A. Glezer, "A high-speed, compressible synthetic jet," *Phys. Fluids* **18**, 017107 (2006).

⁴D. A. Lockerby and P. W. Carpenter, "Modeling and design of microjet actuators," *AIAA J.* **42**, 220 (2004).

⁵R. R. Rathnasingham and K. S. Breuer, "Coupled fluid-structural characteristics of actuators for flow control," *AIAA J.* **35**, 832 (1997).

⁶L. L. Beranek, *Acoustics* (Acoustical Society of America, Melville, NY, 1993), p. 132.

⁷R. K. Shah and A. L. London, "Laminar flow forced convection in ducts," in *Advances in Heat Transfer*, edited by R. F. Irvine and J. P. Hartnett (Academic, New York, 1978), pp. 98, 199.

⁸W. M. Kays and A. L. London, *Compact Heat Exchangers* (McGraw-Hill, New York, 1984), Chap. 5.